

# The collapse of turbulence in the evening

**B.J.H. Van de Wiel<sup>1</sup>, A. F. Moene<sup>2</sup>, H.J.J. Jonker<sup>3</sup>, P. Baas<sup>4</sup>, S. Basu<sup>5</sup>,  
J. Sun<sup>6</sup>, and A.A.M. Holtslag<sup>2</sup>**

<sup>1</sup> *Fluid Dynamics Lab., Eindhoven, Technical University, Eindhoven The Netherlands*

<sup>2</sup> *Dept. of Meteorology and Air Quality, Wageningen Univ., The Netherlands*

<sup>3</sup> *Applied Physics (MSP), Delft Technical Univ. The Netherlands*

<sup>4</sup> *Dept. Atm. Res., Roy. Neth. Weather Inst.(KNMI), De Bilt, The Netherlands*

<sup>5</sup> *Dept. Marine, Earth and Atm. Sci., NC State Univ., USA*

<sup>6</sup> *Nat. Centre of Atm. Res, Boulder, CO, U.S.A.*

*This text is a simplified summary of the technical material presented by the first author on the ECMWF-workshop.*

## Abstract

A common experience in everyday weather is the fact that near-surface wind speeds tend to weaken in the evening, particularly in fair weather conditions. This cessation of wind usually coincides with the collapse of turbulence which leads to a quiet flow near the ground. As the absence of turbulent mixing leads to cold extremes, its prediction is vital for reliable winter temperature forecasts. It is, for example, well-known that unexpected frost events can completely deregulate winter traffic and enhances the risk on calamities (Fig. 1). Yet, the physical explanation behind this phenomenon remained unknown so far. Here, we present a mechanism to explain this intriguing phenomenon by combining extensive observational analysis with new theoretical insights. We detected a remarkable constraint in the kinetic energy of the flow in response to nocturnal cooling. In turn, this results in a limit on the maximum heat that can be transported towards the earth's surface. When the actual heat loss at the surface exceeds this maximum turbulence cannot survive the intense density stratification. By using this insight, a simple predictive tool is developed. This modeling tool shows to be successful in predicting the cessation of turbulence as observed in a unique data set from a 200m meteorological tower covering 10-years of observations.

## 1. Introduction

During day-time turbulent mixing is driven by wind shear and by thermals that form due to solar heating of the earth's surface. In contrast, for the nocturnal case, wind-driven turbulent mixing is largely suppressed by a stably stratified temperature structure: due to net long wave radiative cooling of the surface the air near the surface is relatively cold and dense and is therefore reluctant to move vertically<sup>2-4</sup>. The tendency of the air to 'stick' to the surface is beautifully visualized in cases of thin morning fog<sup>3</sup>. Cold, stable boundary layers not only occur during nighttime, but they also prevail in general arctic and winter conditions, where global warming is expected to be largest<sup>6</sup>. Unfortunately, the description of turbulent mixing under those conditions is highly uncertain in present-generation weather and climate models. Different plausible mixing schemes lead to considerable differences in predicted surface temperatures in the order of 5 to 10 K<sup>7, 8</sup>. One of the problems for physical consistent schemes is to assess whether the cold near-surface air is still able to mix with the warmer air aloft or not. In absence of a rational basis to predict the existence of turbulence, usually so-called 'enhanced mixing procedures' are invoked in forecasting models, in order to tune large-scale performance<sup>7-12</sup>. Clearly, those artificial schemes are physically unrealistic and consequently warm

surface temperature biases are predicted locally during cold extremes<sup>7, 8</sup>. In the present work we reveal the physical mechanism by which the atmosphere decides to remain turbulent or not. From this theoretical framework a conceptual model is developed which is used to predict the collapse of turbulence. The model is successful in predicting existence of turbulent and non-turbulent nights as observed at the 200m meteorological tower at Cabauw in The Netherlands<sup>13</sup>, which covers 10 years of observations.

The existence or absence of nocturnal turbulence in nature is a result of competition between radiative cooling of the surface and downward mixing of warm air. Kinetic energy for this mixing is ultimately provided by the large-scale winds<sup>14</sup>. In Figure 2a, 400 clear nights were subdivided into four classes of geostrophic wind forcing. Because clear nights usually are subject to similar radiative forcing, wind forcing is decisive on the existence of turbulence. Figure 2a shows the sensitivity of turbulent stress (a proxy for turbulent intensity) to wind around sunset. Generally, the intensity of turbulence decreases for all cases due to the decay of convection at the end of the day<sup>15-17</sup>. Interestingly, response is strongly non-linear: a decrease of the 9 m/s wind by a factor 3 does not imply that the stress attains a third of its original value. Moreover, nocturnal turbulent intensity tends to become negligibly small for winds below 3-6 m/s. Here, this intriguing phenomenon is explored and explained. For clarity reasons, we note that aspects of ‘intermittency’ (sporadic, externally triggered turbulent disturbances<sup>4, 5</sup>), that may occur during ‘quiet periods’, are not considered in the present text.



Figure 1: Unexpected road-frost events may cause calamities in traffic (Foto: Kees Slik).

## 2. The heat flux maximum

In essence, turbulent transport can be seen as a gradient-driven diffusion process. This can be summarized in discretized form as<sup>18-20</sup>:  $H \sim K(Ri) \cdot \Delta T / \Delta z$ , with  $H$  the heat transport towards the surface,  $\Delta T / \Delta z$  the vertical gradient of (potential) temperature and  $K(Ri)$  the so-called eddy diffusivity. The latter is a decreasing function of the so-called Richardson number, which represents the competition between the stabilizing temperature gradient and the destabilizing wind shear across the turbulent layer:  $Ri \propto \Delta T / U^2$ . At first instance, we will assume that the velocity at some height above the surface maintains a *fixed* value  $U$ . As will be shown below, this assumption is crucial in the

conceptual model. With constant velocity, the heat flux becomes a function of the temperature gradient only. For small temperature gradients the heat flux tends to zero (gradient limited transport). On the other hand, for large temperature gradients, the heat flux tends to zero as well, but now due to small eddy diffusivity values (mixing limited transport;<sup>22, 23</sup>). In between those extremes a maximum flux level appears. Figure 2b depicts this ‘parabolic’ dependence for both a strong wind (8 [m/s]) and a weak wind case (5 [m/s]). In addition to the heat *supply* by the wind, the energy *demand* is given for an idealized clear and cloudy case. The demand is determined by net long wave radiative cooling of the surface which is largest under clear sky conditions. If low-level clouds are present, they enhance downward long wave radiation and counteract the radiative heat loss<sup>4</sup>. To prevent excessive surface cooling, the energy demand should be balanced by the supply. The black and the grey dots represent thermal equilibria for the clear and cloudy case respectively. In case of clouds, a balance can be reached even with weak winds. In contrast, the limited heat transport in case of weak winds is insufficient to compensate the heat loss under clear sky conditions. Consequently, the surface will start to cool rapidly. In turn, this enhanced cooling will hamper turbulent mixing even more so that eventually all turbulence activity will be suppressed (positive feedback).

In a mathematical sense, the duality of the heat flux depicted in figure 2b has been known over 40 years<sup>21-25</sup>. Yet, this has not led to a comprehensive collapse theory. The reason for this lies in the fact that the underlying assumption of fixed velocity is physically incorrect for atmospheric flows<sup>9, 11, 25</sup>. In equilibrium, large-scale pressure forces are balance by turbulence stresses. In case of ceasing turbulence, frictional forces tend to vanish as well. Consequently, the net force accelerates the flow and finally the boundary layer is able to recover to a turbulent state again (observe the strong sensitivity to wind speed in Figure 2b). Due to this feedback the assumption of constant wind speed is fundamentally flawed and atmospheric boundary layers attain an unconditionally turbulent state in the long term<sup>9, 11, 25</sup>. So then, why do quasi-laminar evening boundary layers seem to be omnipresent in nature?

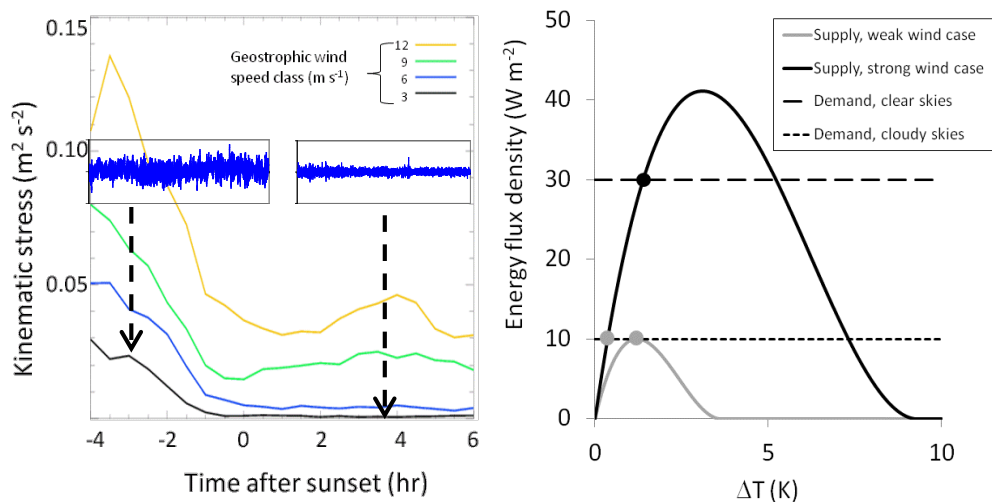


Figure 2: (A) Time evolution of kinematic stress at the KNMI Cabauw observatory (5m level). The curves represent median stress levels for four geostrophic wind classes ( $\pm 1 \text{ m s}^{-1}$ ), as indicated in the graph. Typical vertical velocity fluctuations (10 Hz) are indicated as illustration of turbulent and ‘quiet’ periods. (B) Conceptual graph of the surface energy balance terms (surface heat demand and supply) as a function of the temperature difference between the air mass at 40m and the surface. The dots represent potential equilibria for situations with different ‘external forcings’ related to radiation and wind (see: text).

### 3. The collapse mechanism

Here, we solve this paradox by studying the momentum dynamics in numerical simulations of an idealized channel flow<sup>16</sup>. Figure 3a depicts the evolution of surface stress in response to different cooling rates (denoted by:  $h/L$ ). The initial flow state is neutral. For strong cooling ( $h/L > 1.14$ ), a temporary collapse of turbulence occurs. For moderate cooling, turbulence is able to avoid such collapse. The dashed lines in Figure 3b show the simulated velocity profiles for  $h/L = 1.01$  at snap-shot times corresponding to the colored arrows in 3a. The temporary reduced boundary layer friction causes a significant acceleration. In the end state (3b, red dashed line), the velocity shear is large enough to generate enough turbulent friction to balance the pressure force again (the ‘recovery’ in Fig. 3a). The system is attracted to a turbulent end-state and an analytical theory for the equilibrium velocity profile was developed in agreement with numerical simulations (red full line).

However, whether the system will or will not collapse *in the short-term*, depends on its transient behavior. Unfortunately, in absence of standard methodologies, an analogue mathematical description of transient profiles is usually difficult to find (if possible;<sup>26</sup>). Here, such theory could be developed after the discovery of a remarkable feature in the velocity dynamics. It appears that the profile at the moment of minimal stress intersects with the initial profile (blue dashed and black lines in 3b). Analysis shows that this ‘*velocity crossing point*’ has a strong tendency to remain at a fixed position during the initial, transient phase. The mere existence of this point leads to the crucial insight that our ‘fixed-velocity collapse hypothesis’ must be at play in pressure-driven flows as well.

It was proved that the presence of such a velocity crossing point is due to the conservation of initial momentum in the lower part of the domain. This, in turn, emerges from the fact that the diffusion time-scale is typically much smaller than the acceleration time-scale. As a result a *pseudo-steady* layer develops where the flow is able to reach a temporary, pseudo-equilibrium in accordance with both the

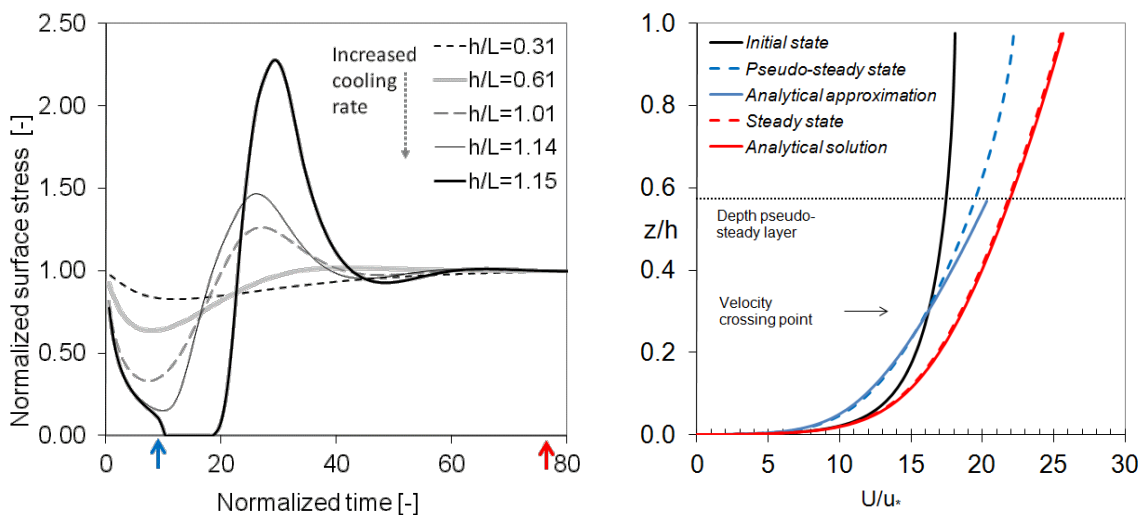


Figure 3: (A) Evolution of surface stress in response to different cooling rates ( $h/L$ -values) in idealized channel flow simulations. The colored arrows indicate the times for which the profiles in figure 3b are given. (B) Velocity profiles (normalized by the friction velocity) The black line represents the initial profile and the red-dotted line the equilibrium state. The blue-dotted line represents the profile at minimal turbulence intensity. The theoretical predictions are given by the full colored lines (see: text). Also the predicted depth of the pseudo-steady layer is indicated.

initiated surface cooling and the initial momentum of the flow. It depends on the magnitude of those competing ‘externals’ whether or not turbulence will be able to survive on the short-term. To state it otherwise: the initial available kinetic energy puts a limit on the maximum heat transport. In analogy to the long-term solutions, analytical solutions were developed for the pseudo-steady state (full blue line). For all cases, the analytical profiles (valid in the lower domain only) are in agreement with the numerical simulations and the height and magnitude of the crossing is predicted correctly. The analytical relations dictate the ‘solution space’<sup>25</sup> for cooling rates that allow a turbulent pseudo-steady state. As such, the theory now provides a physically consistent framework to predict the collapse of turbulence in a channel flow.

#### 4. Atmospheric application and conclusions

It can be anticipated that a similar mechanism will be at play in the atmosphere: due to the sudden reduction of turbulent friction in the evening transition, high-level winds (say  $> 100$  m) accelerate and generate a Boundary Layer Jet<sup>8, 26-28</sup>. At the same time near-surface winds (say  $< 20$  m) weaken<sup>27-29</sup>. Consequently, at intermediate levels (say between  $\sim 30$  and  $60$  m), the wind speed tends to remain constant in time<sup>30</sup>. From observational data analysis it appears that the ‘velocity crossing point’ at Cabauw is located around the  $40$  m level. This fact is used below. Figure 2b showed that for clear-sky conditions only strong winds may support a steady heat balance. An imaginary stepwise decrease in wind speed would lead to a limiting case where the supply line just touches the demand. Obviously, this critical wind in Figure 2 lies in between the  $5$  and  $8$  m/s. By following a similar philosophy a conceptual prediction model was developed and compared with observations from the Cabauw Observatory (Methods Summary; <sup>13</sup>).

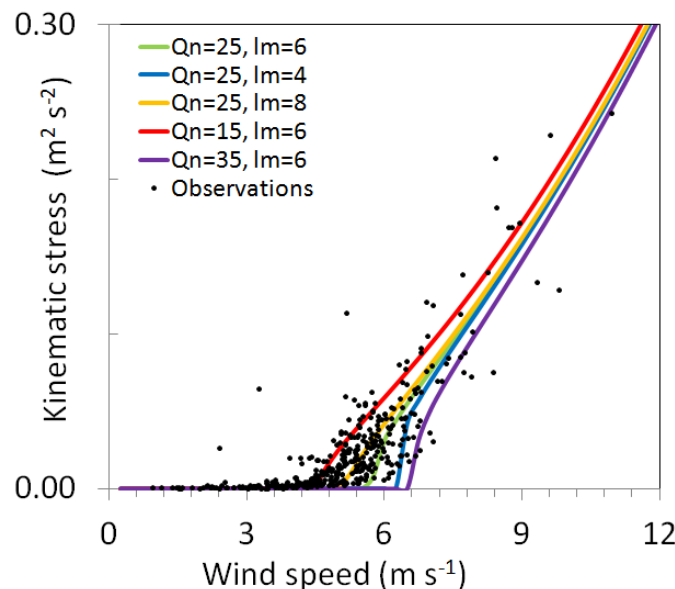


Figure 4: 4-Hour averaged turbulent stress for non-cloudy nights as a function of the 4-hour averaged  $40$  m wind speed at the Cabauw Observatory (see: methods). The curves represent a model sensitivity study under various realistic parameter choices with respect to net radiative cooling ( $Q_n$ ; here defined positive ( $W m^{-2}$ )) and atmosphere-surface coupling ( $l_m$ ; ( $W m^{-2} K^{-1}$ )). Note that both stronger radiative cooling and weaker coupling (to warmer (!) soil) results in higher wind speed thresholds.

In figure 4 each point represents a 4-hour average of turbulent stress during a particular evening as a function of the 40m wind speed (i.e. ~at the assumed crossing point). As anticipated, a minimum speed is needed to maintain significant turbulence. Figure 4, shows the outcome of a sensitivity study where model input parameters related to the radiative cooling and the strength of the atmosphere-surface coupling were varied. Although some variation in the threshold occurs (e.g. stronger cooling require higher speeds to sustain turbulence), a striking qualitative resemblance with the observational characteristics is found. This robustness can be explained from the fact that the maximum sustainable heat flux is proportional to the cube of wind speed, which supports an ‘on-off’ reaction in response to wind forcing. The theory also predicts a (near) logarithmic relation between the threshold and the height of the crossing point. Interestingly, this fact appears to be confirmed by Sun et al. (2011; <sup>5</sup>) who analysed multi-level turbulence observations over the Great Plains (U.S). Although aspects of stationarity were not considered, their results show a clear logarithmic-type of height-dependence with respect to the wind threshold. This suggests that the proposed mechanism has potential general validity in nocturnal boundary layers, and more datasets with various land use characteristics will be explored. We conclude that our conceptual model provides a physically consistent tool in order to forecast the cessation of turbulence.

## Acknowledgements

We are thankful to the Royal Netherlands Weather Institute (KNMI), in particular to Dr. Fred Bosveld, for having provided us with the atmospheric observational data used in figures 2 and 4. We also acknowledge comments on an earlier manuscript by Dr. Larry Mahrt.

## Appendix: Methods Summary

A 10-years dataset is used from the Cabauw observatory<sup>13</sup>, operated by the Royal Netherlands Meteorological Institute. The site is situated over homogeneous grassland. To guarantee stationary, cloud-free synoptic conditions, the following selection criteria were applied: selected night show less than 5 m/s variation of the geostrophic wind between 12 and 00UTC with net longwave radiation at the surface continuously larger than 20 W/m<sup>2</sup> in magnitude. The geostrophic wind was obtained by analyzing surface pressure observations from eight synoptic stations in a radius of 75 km around Cabauw. Turbulent fluxes were obtained using an eddy-covariance technique, applied to 10 Hz data from a sonic anemometer operated at 5 m above ground level. For Figure 2a the average geostrophic wind between 12 and 00UTC was determined for each night. Four geostrophic wind classes ( $\pm 1$  m/s) were defined and for each class the corresponding median stress value is given. In the graph, sunset is defined as the hour at which the shortwave incoming radiation becomes zero. To eliminate effects of varying nighttime length, figure 2a is restricted to the interval -4 to 6 h relative to sunset.

In the theoretical analysis, a channel flow is simulated numerically by solving the conservation equations of heat and momentum in the vertical dimension (assuming horizontal homogeneity), using a stretched grid with 100 discretization levels. Turbulent transport is parameterized by adopting an eddy diffusivity approach (so-called Boussinesq-hypothesis). The turbulence closure assumption uses classical local similarity theory, which is founded on vast observational evidence (see references in the main text) and accounts for both wall and stratification effects. The closure assumption was successfully validated against 3-D Direct Numerical Simulations for this channel flow in Van de Wiel

et al. (2008). The flow has a stress-free boundary condition at the top and no-slip boundary condition at the bottom.

## References

- 1 Edwards, J. M., 2009: Radiative processes in the stable boundary layer: part I Radiative aspects. *Bound. Layer Meteor.*, 131, 105-126.
- 2 Mahrt, L., and D. Vickers, 2006: Extremely weak mixing in stable conditions. *Bound. Layer Meteor.*, 119, 19-39.
- 3 Mahrt, L., Thomas, C., and Heald, R., 2010: Submeso motion visualized by natural and machine generated fog. <http://www.youtube.com/watch?v=8fu1bvGIF44>
- 4 Van de Wiel, B. J. H., A. F. Moene, O. K. Hartogensis, H. A. R. De Bruin, and A. A. M. Holtslag, 2002: Intermittent turbulence and oscillations in the stable boundary layer. Part III: A Classification for observations during CASES99. *J. Atmos. Sci.*, 60, 2509-2522.
- 5 Sun, J., et al., 2011: *J. Atmos. Sci.*, doi: <http://dx.doi.org/10.1175/JAS-D-11-082.1>
- 6 Intergovernmental Panel on Climate Change (IPCC), *Climate change: the physical science basis. Summary for policy makers* (WMO/UNEP) (2007)
- 7 Beljaars, A. C. M., and P. Viterbo, 1998: Role of the boundary layer in a numerical weather prediction model. *Clear and Cloudy Boundary Layers*, Holtslag A. A. M., P. G. Duynkerke, and P. J. Jonker Eds., Royal Netherlands Ac. Of Arts and Sci., Amsterdam, 287-304.
- 8 Svensson et al., 2011: Evaluation of the Diurnal Cycle in the Atmospheric Boundary Layer Over Land as Represented by a Variety of Single-Column Models: The Second GABLSExperiment, *Bound. Layer Meteor.*, 140, 177-206.
- 9 Derbyshire, S. H., 1999a: Stable boundary layer modelling: established approaches and beyond. *Bound. Layer Meteor.*, 90, 423-446.
- 10 Mahrt L., 1998: Stratified atmospheric boundary layers and breakdown of models, *Theoret. Comput. Fluid Dynamics*, 11: 263-279.
- 11 Derbyshire, S. H., 1999b: Boundary-layer decoupling over cold surfaces as a physical boundary instability. *Bound. Layer Meteor.*, 90, 297-325.
- 12 Nappo, C. J., and P-E Johansson, 1999: Summary of the Lövånger international workshop on turbulence and diffusion in the stable planetary boundary layer. *Bound. Layer Meteor.*, 90, 345-374.
- 13 Van Ulden, A. P., and Wieringa, J., 1996: Atmospheric boundary layer research at Cabauw. *Bound. Layer Meteor.*, 78, 39-69.
- 14 Van de Wiel, B. J. H., A. F. Moene, R. J. Ronda, H. A. R. De Bruin, and A. A. M. Holtslag, 2002b: Intermittent turbulence and oscillations in the stable boundary layer. Part II: A system dynamics approach. *J. Atmos. Sci.*, 59, 2567-2581.
- 15 Mahrt, 2011: The near calm stable boundary layer. *Bound. Layer Meteor.*, DOI 10.1007/s10546-011-9616-2.



- 16 Nieuwstadt, F. T. M., 2005: Direct numerical simulation of stable channel flow at large stability. *Bound. Layer Meteor.*, 116, 277-299.
- 17 Flores, O., and J. J. Riley, 2010: Analysis of Turbulence Collapse in the Stably Stratified Surface Layer Using Direct Numerical Simulation. *Bound. Layer Meteor.*, 139, 241-259.
- 18 Businger, J. A., J. C. Wyngaard, Y. Izumi, and E. F. Bradley, 1971: Flux-profile relationships in the atmospheric boundary layer. *J. Atmos. Sci.*, 30, 788-794.
- 19 Högström, U., 1996: Review of some basic characteristics of the atmospheric surface layer. *Bound. Layer Meteor.*, 78, 215-246.
- 20 Grachev, A. A., E. L. Andreas, C. W. Fairall, P. S. Guest, and P. O. G. Persson, 2007: SHEBA flux-profile relationships in the stable atmospheric boundary layer. *Bound. Layer Meteor.*, 124, 315-333.
- 21 Taylor, P. A., 1971: A note on the log-linear velocity profile in stable conditions. *Quart. J.R. Met. Soc.*, 97, 326-329.
- 22 De Bruin, H. A. R., 1994: Analytic solutions of the equations governing the temperature fluctuation method. *Bound. Layer Meteor.*, 68, 427-432.
- 23 Mahrt L., J. Sun, W. Blumen, T. Delany, and S. Oncley, 1998: Nocturnal boundary layer regimes. *Bound. Layer Meteor.*, 88, 255-278.
- 24 Malhi, Y. S., 1995: The significance of the dual solutions for heat fluxes measured by the temperature fluctuation method in stable conditions. *Bound. Layer Meteor.*, 74, 389-396.
- 25 Van de Wiel, B. J. H. , Moene A. F., Steeneveld G. J., Hartogensis O. K., Holtslag A. A. M., 2007: Predicting the Collapse of Turbulence in Stably Stratified Boundary Layers. *Flow Turbulence and Combust.*, 79, 251-274.
- 26 Kundu, P. K., and I. M. Cohen, 2008: *Fluid Mechanics.*, Academic Press, Amsterdam.
- 27 Banta, R. M., L. Mahrt, D. Vickers, J. Sun, B. B. Balsley, Y. L. Pichugina, and E. J. Williams, 2007: The very stable boundary layer on nights with weak low level jets., *J. Atmos. Sci.* 64, 3068-3090.
- 28 Poulos et al., 2002: CASES-99: A comprehensive investigation of the stable nocturnal boundary layer. *Bull, Amer. Meteor. Soc.*, 83, 555-581.
- 29 Lapworth, A., 2008: The evening wind. *Weather*, 63, 12-14.
- 30 Wieringa, J., 1989: Shapes of annual frequency distributions of wind speed observed on high meteorological masts, *Bound. Layer Meteor.*, 47, 85-110.